JOURNAL OF VIROLOGY, Dec. 1987, p. 3950–3959
0022-538X/87/123950-10$02.00/0

Vol. 61, No. 12

The Cellular Secretory Pathway Is Not Utilized for Biosynthesis, Modification, or Intracellular Transport of the Simian Virus 40 Large Tumor Antigen

DONALD L. JARVIS,† WAI-KIT CHAN,‡ MARY K. ESTES, AND JANET S. BUTEL*
Department of Virology and Epidemiology, Baylor College of Medicine, Houston, Texas 77030

Received 26 May 1987/Accepted 20 August 1987

Unlike most proteins, which are localized within a single subcellular compartment in the eucaryotic cell, the simian virus 40 (SV40) large tumor antigen (T-ag) is associated with both the nucleus and the plasma membrane. Current knowledge of protein processing would predict a role for the secretory pathway in the biosynthesis and transport of at least a subpopulation of T-ag to account for certain of its chemical modifications and for its ability to reach the cell surface. We have examined this prediction by using in vitro translation and translocation experiments. Preliminary experiments established that translation of T-ag was detectable with as little as 0.1 μg of the total cytoplasmic RNA from SV40-infected cells. Therefore, by using a 100-fold excess of this RNA, the sensitivity of the assays was above the limits necessary to detect the theoretical fraction of RNA equivalent to the subpopulation of plasma-membrane-associated T-ag (2 to 5% of total T-ag). In contrast to a control rotavirus glycoprotein, the electrophoretic mobility of T-ag was not changed by the addition of microsomal vesicles to the in vitro translation mixture. Furthermore, T-ag did not undergo translocation in the presence of microsomal vesicles, as evidenced by its sensitivity to trypsin treatment and its absence in the purified vesicles. Identical results were obtained with either cytoplasmic RNA from SV40-infected cells or SV40 early RNA transcribed in vitro from a recombinant plasmid containing the SP6 promoter. SV40 early mRNA in infected cells was detected in association with free, but not with membrane-bound, polyribosomes. Finally, monensin, an inhibitor of Golgi function, failed to specifically prevent either glycosylation or cell surface expression of T-ag, although it did depress overall protein synthesis in TC-7 cells. We conclude from these observations that the constituent organelles of the secretory pathway are not involved in the biosynthesis, modification, or intracellular transport of T-ag. The initial step in the pathway of T-ag biosynthesis appears to be translation on free cytoplasmic polyribosomes. With the exclusion of the secretory pathway, we suggest that T-ag glycosylation, palmitylation, and transport to the plasma membrane are accomplished by previously unrecognized cellular mechanisms.

Simian virus 40 (SV40) is a small, nonenveloped virus that productively infects some cell types and can transform others (reviewed in reference 80). The double-stranded DNA genome of SV40 encodes a polypeptide, large tumor antigen (T-ag), that provides many different functions required for viral infection or transformation (reviewed in references 6 and 61). One possible molecular basis for the multifunctional capacity of T-ag is suggested by its unusual dual subcellular distribution (reviewed in references 6 and 61). Most (≥95%) of the intracellular T-ag is localized within the nucleus (nT-ag), whereas the remainder is found at the cell surface in association with the plasma membrane (pmT-ag).

Recent studies have shown that T-ag contains a signal that is required for its nuclear localization and can induce the nuclear localization of heterologous, non-nuclear proteins (33, 34, 44, 45). The identification of this signal represents a key step toward the elucidation of the mechanism by which T-ag is transported to the cell nucleus. In contrast, we know virtually nothing of the mechanism by which a minor subpopulation of T-ag escapes nuclear localization and, instead, becomes localized at the plasma membrane.

Typically, the biosynthesis and transport of plasma-membrane-bound proteins are accomplished by the secretory pathway (reviewed in references 63, 84, and 86). This pathway involves the cotranslational insertion of nascent protein into the membrane of the rough endoplasmic reticulum (RER), a process that is partially mediated by a characteristic stretch of amino acids known as the signal sequence. The newly synthesized protein moves from the RER to the Golgi apparatus and, ultimately, to the plasma membrane. Various co- and posttranslational modifications, such as N-glycosylation, O-glycosylation, and fatty acid acylation, including both myristylation and palmitylation, occur en route (reviewed in references 23, 37, 40, and 69). Some properties of T-ag suggest that the secretory pathway might be involved in its biosynthesis and transport, whereas others suggest that it is not involved.

It appears that at least a subpopulation of pmT-ag spans the plasma membrane. Immunological studies have shown that epitopes on opposite ends of the T-ag molecule are exposed on the surfaces of intact cells (2, 12, 21, 22, 64, 85), and solubility studies suggest that radioiodinatable surface T-ag is associated with the plasma membrane lamina (39). In addition, T-ag undergoes glycosylation (27, 70, 72), and a subpopulation of pmT-ag undergoes palmitylation (38). At first, these properties would seem to be consistent with a model in which T-ag would enter the secretory pathway by insertion into the membrane of the RER and would be glycosylated or palmitylated or both as it travels through the

* Corresponding author.
† Present address: Department of Entomology, Texas A&M University, College Station, TX 77843.
‡ Present address: Cold Spring Harbor Laboratory, Cold Spring Harbor, NY 11724.

RER and Golgi apparatus. However, this model is difficult to reconcile with other known features of T-ag. First, the vast majority of the intracellular T-ag is quickly transported to the nucleus (44, 67, 71). Although it is possible that a structural difference provides a sorting signal that specifically redirects the pmT-ag subpopulation into the secretory pathway, recent comparisons of nT-ag and pmT-ag revealed no such differences (28). Second, the amino acid sequence of T-ag lacks a typical signal sequence (reviewed in reference 6), precluding the most well-documented means of entering the secretory pathway. Third, although T-ag contains a consensus N-glycosylation site (26), it does not undergo N-glycosylation (27, 72), suggesting that it is not exposed to oligosaccharyl transferase in the lumen of the RER (40). That this site is available for glycosylation was shown by a study in which T-ag was forced into the secretory pathway by virtue of a heterologous signal sequence; a chimeric T-ag molecule, equipped with the amino-terminal signal sequence of the influenza hemagglutinin (HA), underwent N-glycosylation (73). Interestingly, the chimeric protein did not undergo normal movement to the cell surface, providing further indirect evidence that the secretory pathway is not normally involved in the biosynthesis and transport of wild-type (WT) T-ag (73).

In this study, we have used a variety of in vitro and in vivo approaches to examine directly the role of the secretory pathway in the biosynthesis and processing of SV40 T-ag. The results show that the secretory pathway is not involved. This finding suggests that previously unrecognized mechanisms exist for the glycosylation, acylation, and intracellular transport of T-ag and probably of other eucaryotic proteins as well.

MATERIALS AND METHODS

Cells and viruses. TC-7 cells, a clonal derivative of the CV-1 line (62), were grown in an enriched minimal essential medium (GIBCO Laboratories, Grand Island, N.Y.) as previously described (54). MA104 cells were grown in medium 199 (GIBCO) supplemented with 5% fetal bovine serum, 0.03% glutamine, 0.075% sodium bicarbonate, 100 U of penicillin per ml, and 100 μg of streptomycin per ml (17).

The Baylor strain of WT SV40 (77) was passaged at low multiplicity of infection and plaque assayed in TC-7 cells (55). The Indiana strain of WT vesicular stomatitis virus (VSV) was passaged and assayed in TC-7 cells as described for SV40, except that the infected cells were not freeze-thawed. Clone 3 of the simian rotavirus SA11 (16) was passaged at low multiplicity of infection and plaque assayed in MA104 cells (17).

Antisera. Normal hamster serum was purchased from PelFreeze Biologicals (Rogers, Ark.). Hamster ascitic fluid (HAF), a polyclonal antiserum with strong reactivity against SV40 T-ag, was prepared as previously described (42). Monospecific guinea pig antiserum against the gel-purified outer capsid glycoprotein of SA11 (αVP7) has been described previously (13). Rabbit antiserum against purified VSV (αVSV) was generously provided by T. Morrison.

Preparation of total cytoplasmic RNA from SV40-infected cells. Confluent TC-7 monolayers were infected with SV40 at a multiplicity of infection of about 50 PFU/cell and treated with 20 μg of cytosine arabinoside (Sigma Chemical Co., St. Louis, Mo.) per ml from 5 to 24 h postinfection. The cells were then detached from the culture vessels with 0.04% EDTA and washed, and the cytoplasmic RNA was extracted and purified by the method of Chirgwin and co-workers (9). Briefly, the cells were swollen in cold hypotonic buffer and lysed with 1% (vol/vol) Nonidet P-40, and the nuclei were pelleted by centrifugation for 5 min at 1,000 × *g*. The postnuclear supernatant was adjusted to 0.5% sodium dodecyl sulfate (SDS), and solid CsCl was added to a density of 1.25 g/ml. The extract was then applied to a CsCl cushion (1.75 g/ml), and the RNA was pelleted by centrifugation for 17 h at 36,000 rpm in a Beckman type 50 Ti rotor at 20°C. The RNA pellet was dissolved in TE buffer (10 mM Tris hydrochloride [pH 8.0], 1.0 mM EDTA), ethanol precipitated twice, and redissolved in TE buffer.

Preparation of RNA from free or membrane-bound polyribosomes. TC-7 cells were infected with SV40, treated with cytosine arabinoside, detached from the culture vessels, and washed as described above. The cells were then swollen on ice in 1 mM $MgCl_2$ and homogenized with a tight-fitting pestle in a Dounce homogenizer. The homogenate was centrifuged for 5 min at 1,000 × *g* using an International PR6 centrifuge and rotor model 269 to pellet the nuclei, and the supernatant was harvested and diluted 1:2 with 60% (wt/vol) sucrose in TM buffer (1 mM Tris hydrochloride [pH 7.5], 1 mM $MgCl_2$). Membrane-bound and free polyribosomes were then separated by rate-zonal ultracentrifugation in discontinuous sucrose gradients as described (7, 53). The gradients were hand layered in Beckman Ultraclear tubes (1 by 3.5 in. [ca. 2.5 by 8.8 cm]) in the following order: 3 ml of 60%, 7 ml of 45%, 7 ml of 40%, 10 ml of 30%, and 7 ml of 25% sucrose. Each sucrose solution was prepared by weight-volume percentage in TM buffer, which was also used to fill the tubes. The gradients were then centrifuged for 16 h at 23,000 rpm in a Beckman SW27 rotor at 4°C. The free polyribosomes pelleted, whereas the membrane-bound polyribosomes banded between the 45% and 60% sucrose layers (7). The membrane band was collected by side puncture, the remainder of the gradient was decanted, and the pellet was dissolved in TE buffer. Each fraction was extracted twice with phenol-chloroform, precipitated twice with ethanol, and dissolved in TE buffer.

In vitro synthesis of SV40 early mRNA. The plasmid pSVT-5, consisting of a cDNA copy of T-ag-encoding early mRNA subcloned into the vector pmK16 number 6 (19), was generously provided by Y. Gluzman. The 2.53-kilobase *Avr*II-*Bam*HI fragment was excised from pSVT-5, purified, and ligated with *Xba*I and *Bam*HI doubly digested pSP64 (Promega-Biotec, Madison, Wis.) (41, 52). A bacterial transformant was isolated that contained the desired recombinant plasmid, with the properly oriented T-ag-coding cDNA sequence immediately 3′ to the strong SP6 promoter. This plasmid, termed pSPT, was amplified and purified by alkaline extraction and CsCl density gradient ultracentrifugation (3). The purified plasmid was then linearized with *Bam*HI, and RNA was synthesized by using the Riboprobe (Promega-Biotec) in vitro transcription system according to the instructions of the manufacturer. Aliquots of the 100-μl reaction mixture were used directly for cell-free translation as described below.

Preparation of SA11 RNA. Rotavirus mRNA was synthesized in vitro by using the RNA polymerase activity endogenous to purified virus. The mRNA was isolated from the reaction mixture by phenol-chloroform extraction and ethanol precipitation as previously described (50).

Cell-free translation of RNA. RNA samples were quantitated by A_{260} and translated in a rabbit reticulocyte lysate as previously described by Mason et al. (50). The lysate was prepared by hypotonic shock of washed reticulocytes obtained from anemic rabbits, clarified by centrifugation for 10

min at 27,000 × g, and stored in small samples at −70°C. Prior to use, the lysate was supplemented with 8 μM bovine hemin (Sigma; type I), 10 mM creatine phosphokinase (Sigma; type I), 25 μM amino acids except methionine, 90 mM KCl, 0.5 mM $MgCl_2$, and 1 mM $CaCl_2$ and then was treated with micrococcal nuclease (Sigma). The nuclease was inactivated with ethylene glycol-bis-(β-aminoethyl ether)-*N,N'*-tetraacetic acid, and the treated lysate was further supplemented with 60 μg of wheat germ tRNA (Sigma) per ml. The treated and reconstituted lysate was used immediately or was stored at −70°C for 3 to 4 months.

For cell-free translation, 90 U of RNasin (Promega-Biotec), 25 μCi of [^{35}S]methionine (1,000 to 1,500 Ci/mmol; Amersham Corp., Arlington Heights, Ill.), and various amounts of RNA were added to 90 μl of the lysate, and the mixture was incubated for 1 h at 30°C. The reaction was terminated by RNase treatment, and the samples were diluted to 1 ml with cold extraction buffer (50 mM Tris hydrochloride [pH 8.0], 100 mM NaCl, 1% [vol/vol] Nonidet P-40) containing 200 μM leupeptin (Sigma) (29). The solubilized samples were then clarified and immunoprecipitated as described below.

In some experiments, cell-free translation of RNA was carried out in the presence of canine pancreatic microsomal vesicles (4). The microsomes were prepared by the method of Shields and Blobel (74) as previously described (14) and were stored in 50% glycerol at −70°C. Translations were performed as described above, but with the addition of 3 to 6 A_{280} units of the microsome preparation and 3 mM tetracaine hydrochloride. Samples were immunoprecipitated either immediately after translation or after a 1-h treatment with 100 μg of tolylsulfonyl phenylalanyl chloromethyl ketone-trypsin (Worthington Enzymes, Freehold, N.J.) per ml

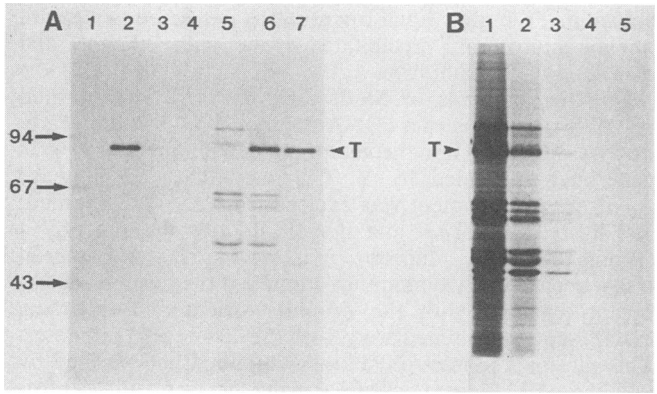

FIG. 1. Characterization of the in vitro translation reaction for T-ag. Cytoplasmic RNA was extracted from SV40-infected TC-7 cells, partially purified, and translated in a cell-free system as described in Materials and Methods. (A) Specificity of the assay. Translations were performed in the absence of exogenous RNA (lanes 3 and 4) or in the presence of 10 μg of RNA (lanes 5 and 6). Samples were then immunoprecipitated with normal hamster serum (lanes 3 and 5) or HAF (lanes 4 and 6), and the immunoprecipitates were washed, disrupted, and analyzed on an 8% acrylamide gel. SV40-infected cell extracts immunoprecipitated with normal hamster serum (lane 1) or HAF (lanes 2 and 7) are shown as controls. This photograph is of an autoradiogram exposed for 2 days. (B) Sensitivity of the assay. Translations were performed with 10 (lane 1), 1.0 (lane 2), 0.1 (lane 3), 0.01 (lane 4), or 0.001 μg (lane 5) of RNA, and the samples were immunoprecipitated with HAF. This photograph is of an autoradiogram exposed for 1 month. Molecular weight markers are given in thousands. The arrow labeled with a T indicates the position of T-ag.

(87). Trypsin digests were performed at 22°C in the presence or absence of 1% (vol/vol) Triton X-100 (Sigma). Alternatively, the reaction mixture was separated into soluble and particulate (microsomal) fractions prior to immunoprecipitation (32). This was accomplished either by centrifugation for 1 h at approximately 13,500 × g in a microcentrifuge (model 235B; Fisher Scientific Co., Pittsburgh, Pa.) or by ultracentrifugation through a high-salt-sucrose cushion (0.5 M sucrose in 20 mM Tris hydrochloride [pH 7.4], containing 500 mM KCl, 2 mM $CaCl_2$, and 5 mM $MgCl_2$) for 45 min at 40,000 rpm in a Beckman SW50.1 rotor.

Metabolic labeling, extraction, and immunoprecipitation. Confluent TC-7 monolayers were infected at high multiplicity of infection with SV40 or VSV and were pulse-labeled with [^{35}S]methionine (Amersham) or D-[1-^{3}H]galactose (50 Ci/mmol; ICN Pharmaceuticals Inc., Irvine, Calif.) as previously described (27). The precise labeling conditions used in individual experiments and the details of inhibitor treatments are noted in the figure legends. After being labeled, the monolayers were washed and extracted with extraction buffer supplemented with leupeptin, and the extracts were clarified. The extracts were then treated with antiserum and fixed *Staphylococcus aureus* Cowan I (36), and the resulting immunoprecipitates were washed and disrupted as previously described (27). The disrupted immunoprecipitates were analyzed by SDS-polyacrylamide gel electrophoresis as previously described (75), and the gels were impregnated with Autofluor (National Diagnostics, Somerville, N.J.), dried, and exposed to Kodak XAR-5 film at −70°C. In some experiments, bands of interest were excised from dried gels and solubilized by the method of Mahin and Lofberg (48), and radioactivity was quantitated by liquid scintillation spectroscopy with a Beckman model LS-250 spectrometer.

Cell surface labeling. Surface proteins of intact cells were labeled by the lactoperoxidase-catalyzed radioiodination method as previously described (49, 76).

RESULTS

Cell-free synthesis of SV40 T-ag. Preliminary experiments were performed to establish the specificity and sensitivity of the cell-free translation reaction for SV40 T-ag (Fig. 1). In the absence of exogenous RNA, no newly synthesized proteins were immunoprecipitated from the reaction mixture, indicating that the level of endogenous protein synthesis was low (panel A, lanes 3 and 4). The addition of cytoplasmic RNA from SV40-infected cells resulted in the synthesis of several proteins, most of which were nonspecifically immunoprecipitated with both normal hamster serum and HAF (panel A, lanes 5 and 6). However, T-ag was the predominant protein product, and it was specifically immunoprecipitated with HAF (panel A, lane 6). As previously reported by Prives et al. (59) and Paucha et al. (58), the electrophoretic mobility of T-ag synthesized in the cell-free system (panel A, lane 6) was identical to that of T-ag synthesized in SV40-infected cells (panel A, lanes 2 and 7); both migrated with an apparent molecular weight of about 90,000. (Although the in vitro product appears to migrate slightly behind the in vivo product in Fig. 1A, this difference was not reproducible and probably resulted from distortion of this particular gel when it was dried.) This result is consistent with the notion that chemical modifications of T-ag that occur in vivo but not in vitro have no detectable influence on its electrophoretic mobility. As previously suggested by Denhardt and Crawford (11), the primary amino acid sequence near the carboxy terminus of T-ag

induces an anomaly in its electrophoretic behavior that appears to override and obscure any effects of modifications.

The rabbit reticulocyte system provided excellent sensitivity, since T-ag was detectably translated from as little as 0.1 μg of the cytoplasmic RNA preparation (Fig. 1B, lane 3). On the basis of this result and previous estimates that the pmT-ag subpopulation comprises about 2 to 5% of the total T-ag (43, 76), we used 10 μg (a 100-fold excess) of RNA for all subsequent cell-free translation experiments. This ensured the detectable translation of a fraction of the input RNA equivalent to the pmT-ag subpopulation. We considered this to be important in case pmT-ag is translated from a subpopulation of SV40 early mRNA that interacts with the early components of the cellular secretory pathway. (In fact, a faint T-ag band was detectable in the original autoradiogram when only 0.01 μg of RNA was used, indicating that the sensitivity of the assay was well within the theoretical required limits.) It must be emphasized, however, that this is strictly a hypothetical possibility; there is no evidence for more than one T-ag-encoding mRNA population.

In vitro translocation of T-ag. The ability of T-ag or the pmT-ag subpopulation to enter the secretory pathway was examined by using two different in vitro translocation assays. The first was a protease protection assay (87) involving the cell-free translation of RNA in the presence of microsomal vesicles, followed by treatment of the reaction mixture with trypsin and analysis by immunoprecipitation and SDS-polyacrylamide gel electrophoresis. With this assay, the protein of interest will be detected only if translocation occurs, because it must enter the microsomal vesicle to be protected from the action of the exogenous protease. The second was a copurification assay (32), in which RNA is translated in the presence of microsomal vesicles, the reaction mixture is separated into soluble and particulate fractions by centrifugation, and each fraction is assayed by immunoprecipitation and SDS-polyacrylamide gel electrophoresis. In this case, the ability of a protein to copurify with the microsomes in the particulate fraction indicates that it has undergone translocation. A viral glycoprotein known to enter the secretory pathway at the level of the RER, VP7 of rotavirus SA11 (reviewed in reference 15), served as a positive control in both assays. Although the rotavirus VP7 is a more heavily glycosylated protein than T-ag, it utilizes a typical mechanism to enter the secretory pathway, and it represented a good indicator that the various assays were behaving properly.

The results of the positive control for the protease protection assay are shown in Fig. 2A. Translation of rotavirus SA11 mRNA in the absence of microsomes resulted in the synthesis of the nonglycosylated precursor to the structural glycoprotein VP7 (lane 1). In the presence of microsomes, the 35,000-molecular-weight precursor was converted to the 38,000-molecular-weight N-glycosylated end product (lane 2). The majority of this protein was translocated across the microsomal membrane, as demonstrated by its resistance to trypsin treatment (lane 3); quantitation of the radioactivity in the VP7 bands seen in lanes 2 and 3 revealed that approximately 70% of the mature protein was protected (data not shown). In addition, solubilization of the vesicles before trypsinization demonstrated that VP7, if accessible, was completely susceptible to digestion by the enzyme (lane 4).

The results of analogous experiments were quite different for SV40 T-ag (Fig. 2B). First, there was no detectable difference in the apparent molecular weight of T-ag synthesized in the absence (lane 1) or presence (lane 2) of microsomal vesicles. Second, T-ag did not cross the membrane of the microsomal vesicles, as evidenced by its complete susceptibility to trypsin digestion in the absence of detergent (lane 3). A 1-month overexposure, which was sufficient to detect T-ag synthesized from only 1% of the RNA used in this experiment (Fig. 1B, lane 3), still revealed no trace of a T-ag band in lane 3 (data not shown). These results suggest that T-ag does not enter the cellular secretory pathway, at least not by translocation across the membrane of the RER.

It was possible, however, that T-ag was translocated, but that only a minimal domain of the molecule crossed the membrane of the microsomal vesicle. If so, most of the molecule would still be accessible for trypsin digestion and an intact T-ag band would not be observed. To address this possibility, we used another approach, the copurification assay, to determine whether T-ag underwent translocation (Fig. 3). Initially, the translation mixture was simply microfuged for 1 h, and the supernatant and pellet fractions were immunoprecipitated for T-ag. T-ag was not detected in association with the microsomal vesicles in the pellet (lane 3) but was quantitatively recovered from the supernatant fluid (lane 2; compare with the unfractionated mixture in lane 1). In a similar but more rigorous experiment, the cell-free translation mixture was ultracentrifuged through a high-salt-sucrose cushion to pellet the microsomes. T-ag failed to copurify with the microsomal vesicles (lane 5); it was recovered from the supernatant fraction (lane 4). In contrast, the mature VP7 glycoprotein copurified with the microsomal

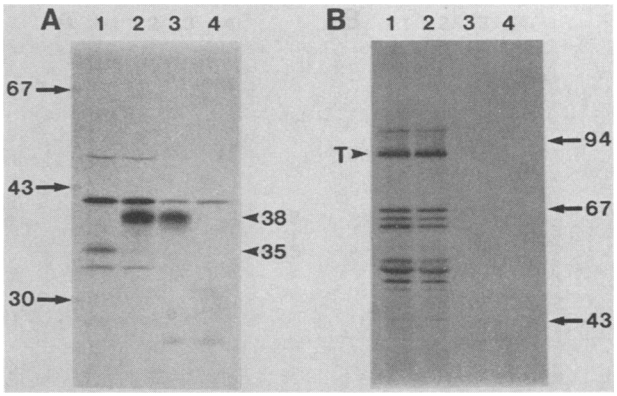

FIG. 2. Protease protection assay for in vitro translocation of SA11 VP7 and SV40 T-ag. SA11 RNA and cytoplasmic RNA from SV40-infected TC-7 cells were prepared as described in Materials and Methods. (A) Samples (40 ng) of SA11 RNA were translated in vitro in the absence (lane 1) or presence (lanes 2, 3, and 4) of microsomal membranes. One sample of each was harvested immediately after translation by immunoprecipitation with αVP7 (lanes 1 and 2). The other samples, both of which had been translated in the presence of microsomes, were treated with 100 μg of trypsin per ml for 1 h at room temperature without (lane 3) or with (lane 4) prior solubilization of the membrane vesicles with Triton X-100. Those samples were then immunoprecipitated as described above, and all immunoprecipitates were washed, disrupted, and analyzed on a 10% polyacrylamide gel. The arrows labeled 35 and 38 indicate the positions of the nonglycosylated precursor and the mature, N-glycosylated forms of VP7, respectively. This photograph is of an autoradiogram exposed for 1 day. (B) Samples (10 μg) of the cytoplasmic RNA from SV40-infected cells were translated in vitro under the same sets of conditions detailed for the SA11 RNA samples. For these samples, however, HAF was used for immunoprecipitation, and the samples were analyzed on an 8% acrylamide gel. This photograph is of an autoradiogram exposed for 2 days. Molecular weight markers are given in thousands.

vesicles through two consecutive high-salt-sucrose cushions (lane 8). As in the protease protection experiment, a 1-month overexposure failed to reveal a T-ag band in the gradient-purified microsomal fraction (lane 5; data not shown). These results support the interpretation that T-ag does not undergo translocation in vitro.

In the preceding experiments, unselected cytoplasmic RNA was used for the cell-free translation of T-ag. Because SV40 early mRNA represents only about 0.1% of the total cytoplasmic RNA in SV40-infected cells (59), it was possible that T-ag failed to undergo translocation because this minor mRNA population was outcompeted for the cellular machinery required to cross the RER membrane. For example, unrelated cellular mRNA species might have effectively occupied all of the signal recognition particle (83) in the lysate or the signal recognition particle receptor sites (18) in the microsomal membranes. To circumvent this possible complication, we constructed a recombinant plasmid (pSPT) in which a cDNA copy of T-ag mRNA was positioned behind an SP6 promoter. This plasmid was used to synthesize essentially pure SV40 early RNA in vitro, which was used, in turn, for in vitro translocation experiments analogous to those described above. Identical results were obtained with these pure mRNA preparations. Translocation of T-ag across the membrane of microsomal vesicles was not detected by either protease protection or copurification assays (Fig. 4).

The results of these studies demonstrate convincingly that SV40 T-ag does not undergo translocation in vitro and suggest that T-ag does not enter the secretory pathway in vivo, at least not at the level of the RER.

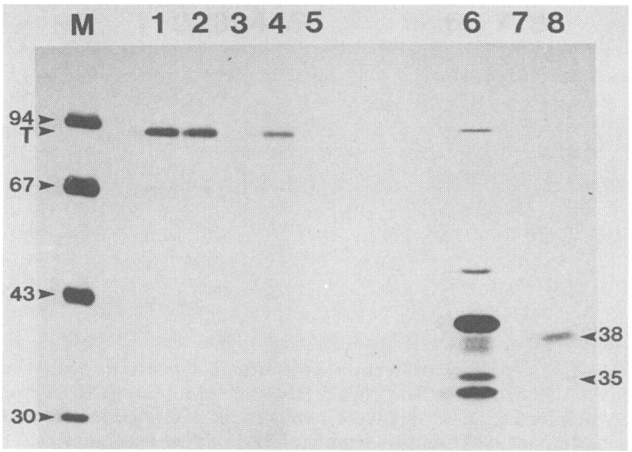

FIG. 3. Copurification assay for in vitro translocation of SA11 VP7 and SV40 T-ag. Samples (10 μg) of cytoplasmic RNA from SV40-infected cells (lanes 1 through 5) or 40-ng samples of SA11 RNA (lanes 6 through 8) were translated in vitro in the presence of microsomal vesicles. One sample of each was harvested immediately after translation by immunoprecipitation with HAF (lane 1) or αVP7 (lane 6). For SV40 RNA only, another sample was centrifuged for 1 h in a Fisher microcentrifuge, and the resulting supernatant (lane 2) and pellet (lane 3) fractions were each immunoprecipitated with HAF. For both SV40 and SA11 RNA, one sample of each was centrifuged through two consecutive high-salt-sucrose cushions as described in Materials and Methods. The supernatant fractions from the first centrifugation were immunoprecipitated with HAF (lane 4) or αVP7 (lane 7), as were the pellets from the second centrifugation (lanes 5 and 8, respectively). The 38,000-molecular-weight doublet in lane 6 shows the two protein products encoded in the bicistronic SA11 RNA segment 9, as previously reported by Chan et al. (8). This photograph is of an autoradiogram exposed for 1 week. Molecular weight markers are given in thousands.

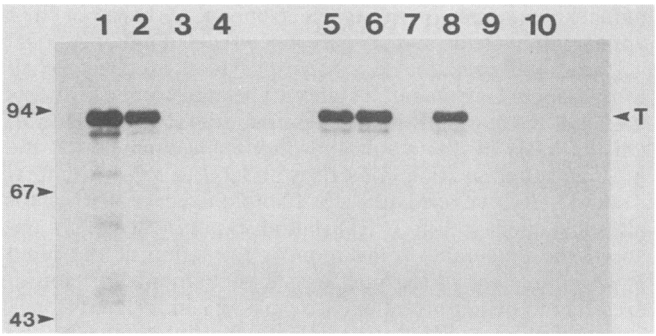

FIG. 4. Translocation assays with in vitro synthesized SV40 early RNA. The RNA for these experiments was prepared by in vitro transcription of a recombinant plasmid containing a cDNA copy of the SV40 early region under the control of an SP6 promoter, as described in Materials and Methods. Lanes 1 to 4 show a protease protection assay equivalent to that performed for lanes 1 to 4 in Fig. 2B. Lane 1, translation of RNA alone; lane 2, translation in the presence of microsomal vesicles; lane 3, translation in the presence of microsomal vesicles followed by trypsin treatment; lane 4, translation in the presence of microsomal vesicles followed by treatment with Triton X-100 and trypsin. Each of the samples was immunoprecipitated with HAF after the indicated treatments. Lanes 5 to 10 show a copurification assay. Three samples of RNA were translated in the presence of microsomal vesicles. One was immunoprecipitated immediately after translation (lane 5). Another was microcentrifuged for 1 h, and the supernatant (lane 6) and pellet (lane 7) fractions were separately immunoprecipitated. The third sample was centrifuged through two consecutive high-salt-sucrose cushions as described in Materials and Methods, and the supernatant (lane 8) and both of the pellets (lanes 9 and 10) were immunoprecipitated. All immunoprecipitates were washed, disrupted, and analyzed on an 8% acrylamide gel. This photograph is of an autoradiogram exposed for 1 day. Molecular weight markers are given in thousands.

In vivo localization of T-ag biosynthesis. If T-ag is synthesized and transported to the cell surface through the secretory pathway, current models of this pathway would predict that at least a subpopulation of the SV40 early mRNA would be translated by membrane-bound polyribosomes. This prediction presented an in vivo approach by which to assess the role of the secretory pathway in T-ag biosynthesis and transport, i.e., free and membrane-bound polyribosomes were purified from SV40-infected cells and examined separately for the presence of SV40 early mRNA by cell-free translation (Fig. 5). RNA extracted from the purified membrane-bound polyribosomes did not result in the translation of detectable T-ag (lane 2), whereas RNA extracted from free polyribosomes purified from the same cells did result in such translation (lane 3). In both cases, 10 μg of RNA was added to the cell-free translation system, but it can be noted that less T-ag was synthesized than with total cell RNA (lane 1). The amount of translatable mRNA in the polysomal RNA preparations was probably less than in the unfractionated RNA preparation, presumably because of RNA degradation during cellular fractionation procedures. The important comparison in this experiment was between the two polysome fractions, rather than between fractionated and unfractionated RNA, and we assumed that such degradation would be comparable in the two fractions. Fortunately, since this separation enriched for RNA in the membrane-bound fraction that would give translocatable products, the sensitivity of the assay was effectively enhanced. All the T-ag RNA that

might have been present in the bound fraction should have generated translocatable T-ag, but none was detected. This result suggests that the T-ag in SV40-infected cells is translated by free, and not by membrane-bound, polyribosomes. The failure to detect any viral mRNA in the membrane-bound polyribosome fraction is inconsistent with a role for the secretory pathway in the biosynthesis and transport of this protein to the cell surface. It should be noted that this approach has been commonly used to determine the sites of synthesis of other viral proteins (for examples, see references 7, 53, and 60).

Role of the Golgi apparatus in T-ag biosynthesis and transport. Although the results described above suggested that T-ag does not enter the secretory pathway by translocation across the membrane of the RER, we considered the possibility that it might somehow circumvent this early event and enter the pathway at the level of the Golgi apparatus. Such a mechanism might explain the ability of a subpopulation of T-ag to achieve a plasma membrane localization, as well as its chemical modifications by glycosylation (27, 70, 72) and palmitylation (38). Monensin is a carboxylic ionophore that has been used extensively to investigate the functions of the Golgi apparatus (78). It inhibits O-glycosylation and terminal N-glycosylation events, and it interrupts the transport of certain glycoproteins that are routed through the Golgi apparatus in transit to the plasma membrane (1, 30, 31). We used monensin to assess the functional role of the Golgi apparatus in the biosynthesis and transport of SV40 T-ag.

Initially, we examined the effect of monensin on overall protein synthesis in TC-7 cells. Despite numerous reports that monensin has no adverse effect on cellular protein synthesis in a variety of different cell types, we found that typical monensin treatments inhibited overall protein synthesis in TC-7 cells (Fig. 6). This was not a synergistic effect between the virus infection and the inhibitor treatment, because similar results were obtained with SV40-infected (top panel) and uninfected (bottom panel) cells. The results of monensin experiments, therefore, had to be interpreted cautiously, because any potentially specific effect had to be distinguished from a nonspecific effect due to the general inhibition of T-ag biosynthesis.

The effects of monensin on the overall biosynthesis,

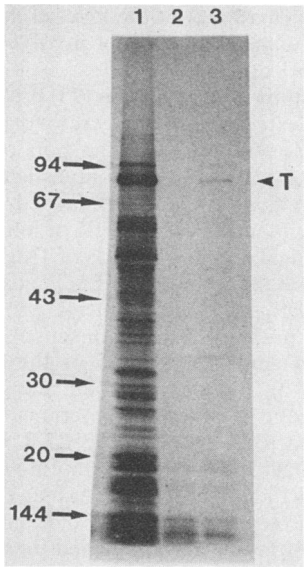

FIG. 5. In vitro translation of RNA isolated from free or membrane-bound polyribosomes of SV40-infected TC-7 cells. Free and membrane-bound polyribosome fractions were prepared from SV40-infected TC-7 cells as described in Materials and Methods. The RNA was isolated from each fraction by phenol-chloroform extraction and ethanol precipitation and was then resolubilized and quantitated. RNA (10 μg) from each fraction was translated in vitro, and the samples were immunoprecipitated with HAF. An immunoprecipitate prepared from in vitro translation of 10 μg of the total cytoplasmic RNA from infected TC-7 cells served as a control (lane 1). Lane 2, RNA from membrane-bound polyribosomes. Lane 3, RNA from free polyribosomes. This photograph is of an autoradiogram exposed for 4 weeks. Molecular weight markers are given in thousands.

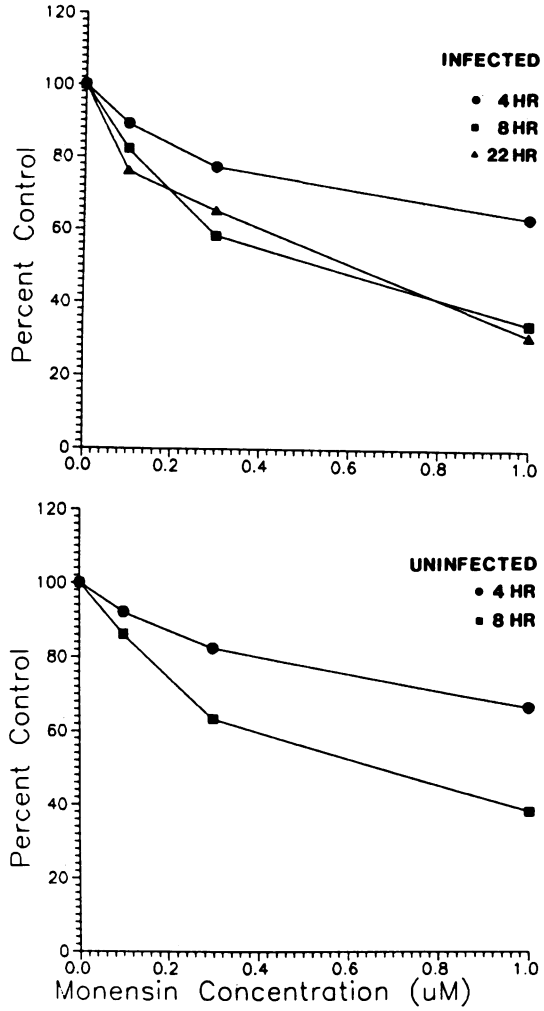

FIG. 6. Effect of monensin treatment on protein synthesis in SV40-infected and uninfected TC-7 cells. Infected or uninfected TC-7 cells were treated with monensin for 4, 8, or 22 h beginning at 20, 16, or 2 h postinfection, respectively. In each case, the cells were starved for 30 min in glucose-free minimal essential medium and then labeled with 10 μCi of [^{35}S]methionine per ml in glucose-free minimal essential medium for the last 3 h of the treatment period. The cells were extracted, extracts were clarified, and triplicate samples of each extract were spotted onto glass fiber filters for trichloroacetic acid precipitation. Each filter was counted in a liquid scintillation spectrometer, background counts were subtracted, and the triplicate values were averaged. All values are expressed as percentages of the corresponding control samples from untreated cells. The average control value for infected cells was 98,354 cpm, as determined from triplicate samples of three different cell extracts. The control value for uninfected cells was 51,967 cpm, as determined from triplicate samples of a single cell extract.

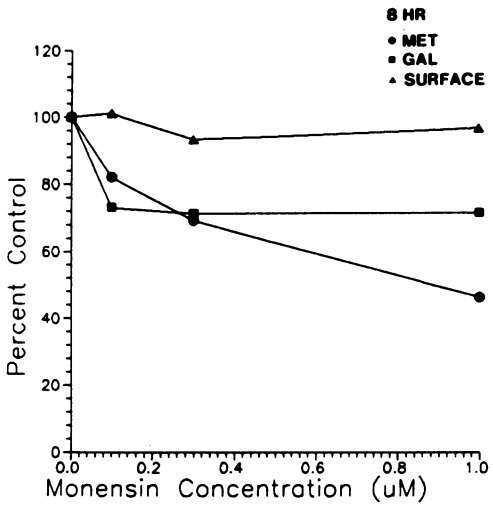

FIG. 7. Effect of monensin on biosynthesis, glycosylation, and surface expression of T-ag. SV40-infected TC-7 cells were treated with monensin for 8 h as described in the legend to Fig. 6. Cells were starved in glucose-free minimal essential medium for 30 min and then were labeled with 10 μCi of [^{35}S]methionine per ml or 100 μCi of [^{3}H]galactose per ml in the same medium for the last 3 h of the treatment period or were surface radioiodinated at the end of the treatment period. The cells were extracted, and clarified extracts were immunoprecipitated with HAF. The immunoprecipitates were washed, disrupted, and resolved on 8% acrylamide gels, and the T-ag bands were located by autoradiography and excised. The gel slices were solubilized by the method of Mahin and Lofberg (48), and radioactivity was determined by liquid scintillation spectroscopy. All values are expressed as percentages of the corresponding control samples from untreated, infected cells. All of the control values were determined as average solubilized counts per minute from T-ag bands obtained from three different cell extracts. These values were 5,910, 1,659, and 844 cpm for methionine-labeled, galactose-labeled, and surface-radioiodinated T-ag, respectively.

glycosylation, and cell surface expression of T-ag were compared under a variety of different treatment conditions. Treated or untreated cells were pulse-labeled with [^{35}S]-methionine or [^{3}H]galactose or were surface iodinated, and the T-ag was extracted, immunoprecipitated, and analyzed by SDS-polyacrylamide gel electrophoresis. Qualitatively, no difference was observed in the electrophoretic mobility of T-ag isolated from treated or untreated cells (data not shown). Quantitatively, no specific inhibition of T-ag glycosylation or cell surface expression was observed; inhibition of both was less than or approximately equal to the background inhibition of overall T-ag synthesis (Fig. 7). Even at monensin concentrations of only 0.01 and 0.1 μM, however, Golgi function was effectively inhibited, as revealed by a very slight increase in the electrophoretic mobility of the G glycoprotein of VSV (VSV-G; data not shown). It has been suggested that this change reflects the inhibition of terminal glycosylation of VSV-G, which normally occurs in the late (*trans*) compartment of the Golgi apparatus (1). Together, these data suggest that a functional Golgi apparatus is probably not required for the glycosylation or cell surface expression of SV40 T-ag.

DISCUSSION

The SV40 T-ag represents a unique and interesting model for the study of protein biosynthesis, modification, and transport in eucaryotic cells. T-ag ultimately achieves a very unusual dual subcellular distribution in both the nucleus and plasma membrane (reviewed in references 6 and 61). In addition, it acquires a large number of different chemical modifications, including N-terminal acetylation (51), phosphorylation at multiple sites (66, 79, 82), poly-ADP ribosylation (20), glycosylation (27, 70, 72), acylation (38), and adenylation (5). Presently, it is not known how or where all of these modifications occur or what influence each might have on the sorting of T-ag molecules, their targeting to different subcellular compartments, or their functional capabilities.

The transit of T-ag to the cell surface, coupled with its modifications by glycosylation and palmitylation, suggested that the secretory pathway might be utilized for T-ag biosynthesis and transport. The secretory pathway represents the most well-characterized mechanism for the specific transport of proteins to the plasma membrane (reviewed in references 63, 84, and 86). Furthermore, proteins are commonly glycosylated and acylated in the organelles that compose this pathway (reviewed in references 23, 37, 40, and 69). Nonetheless, the experimental results described in this report strongly suggest that the secretory pathway is not used for the biosynthesis or subsequent processing of T-ag. Several different assays proved that T-ag does not undergo translocation in vitro, and each was validated by the use of a rotavirus glycoprotein known to enter the secretory pathway through the RER as a positive control. T-ag-encoding mRNA was detected in vivo only in association with free, and not with membrane-bound, polyribosomes. An inhibitor of Golgi function, monensin, failed to specifically prevent the glycosylation of T-ag or its expression at the cell surface. Together, these findings strongly suggest that T-ag does not enter the secretory pathway at the level of the RER and that the Golgi apparatus is probably not involved in the modification or transport of T-ag.

In a previous study, Sharma et al. (73) presented evidence which also suggested that the secretory pathway is not utilized for the biosynthesis and transport of T-ag. Using a recombinant DNA approach, these investigators engineered a chimeric protein, HA-T-ag, composed of the amino-terminal signal sequence from the HA of influenza virus and the carboxy-terminal 694 amino acids of T-ag. The HA signal sequence mediated the transfer of HA-T-ag across the membrane of the RER, and the chimeric protein underwent N-glycosylation, presumably at a consensus recognition site located at amino acids 153 to 155 of the T-ag sequence. However, HA-T-ag did not proceed along the secretory pathway to achieve a plasma membrane localization; instead, it appeared to be stuck in the RER. The two observations, i.e., that HA-T-ag underwent N-glycosylation whereas WT T-ag did not and that HA-T-ag did not reach the plasma membrane whereas WT T-ag did, suggested that the secretory pathway is not normally used for the biosynthesis and transport of WT T-ag.

In summary, the results of this study and the study of Sharma et al. (73) eliminate the secretory pathway as a potential mechanism for the biosynthesis and processing of SV40 T-ag. We now face the task of designing a model to account for the glycosylation, palmitylation, and cell surface transport of T-ag, without invoking the ordinary mechanisms that are known to exist within the confines of the secretory pathway. From our examination of free and membrane-bound polyribosome fractions for the presence of SV40 early mRNA, we can conclude that the first step in the T-ag biosynthetic pathway is its translation on free polyribosomes in the cytoplasm of the cell. This is consistent with the

previous isolation of T-ag-encoding early mRNA from free polyribosomes prepared from SV40-transformed mouse cells (57). The processing events that proceed during and after the biosynthesis of T-ag, however, remain open to speculation and further investigation.

Theoretically, a subpopulation of T-ag could be targeted for transport to the plasma membrane by a unique structural feature, but recent structural comparisons of nT-ag and pmT-ag failed to reveal any differences (28). The sorting process might rely upon a subtle structural difference that we are presently unable to detect, or it might be completely nonspecific. The latter possibility is intellectually unsatisfying, because available evidence suggests that pmT-ag plays an important functional role in SV40-induced cellular transformation (35, 46, 65; reviewed in reference 6). Finally, it is possible that the pmT-ag subpopulation is derived directly from the predominant nT-ag population (28, 73). However, this model would require a novel mechanism of protein transport between the nucleus and plasma membrane, and it cannot account for the presence of pmT-ag in cells infected with a nuclear-transport-defective mutant of SV40 (43).

On the basis of current knowledge of protein acylation mechanisms (69), it is difficult to explain how T-ag would undergo palmitylation outside of the secretory pathway. However, it has been suggested that palmitylation of pmT-ag might occur at the plasma membrane itself by exchange with membrane lipids (47). This proposal is consistent with the present conclusion that the Golgi apparatus is probably not involved in the modification or transport of T-ag. Interestingly, it has recently been noted that most acylated proteins are not N-glycosylated, suggesting that acylated integral membrane proteins may follow different intracellular transport pathways than cell surface glycoproteins (56).

It is equally difficult to envision how T-ag can undergo glycosylation in the absence of the mechanisms available within the secretory pathway. However, a new mechanism that involves the formation of an unusual O-glycosidic bond between *N*-acetylglucosamine and serine or threonine has recently been described (24, 68, 81). In contrast to the secretory pathway, where glycosylation occurs exclusively on the lumenal side of cellular membranes, this glycosylation event appears to occur on the cytoplasmic or nucleoplasmic side of membranes (10, 25; J. A. Hanover, C. K. Cohen, M. C. Willingham, and M. K. Park, submitted for publication). We are currently exploring the exciting possibility that this newly recognized mechanism can explain the enigmatic observation that T-ag can undergo glycosylation without entering the cellular secretory pathway.

ACKNOWLEDGMENTS

We extend our gratitude to T. Morrison and Y. Gluzman for gifts of VSV antiserum and pSVT-5, respectively, and to L. Donehower for advice on the construction of pSPT. We also thank J. Hanover and G. Hart for helpful discussions and for sharing their unpublished results.

This study was supported in part by Public Health Service research grants CA22555 and CA09197 from the National Cancer Institute, by Public Health Service research grant AM30144 from the National Institute of Arthritis, Diabetes and Digestive and Kidney Diseases, and by Public Health Service grant RR-05425 from the National Institutes of Health.

LITERATURE CITED

1. **Alonso-Caplen, F. V., and R. W. Compans.** 1983. Modulation of glycosylation and transport of viral membrane glycoproteins by a sodium ionophore. J. Cell Biol. **97**:659–668.
2. **Ball, R. K., B. Siegl, S. Quellhorst, G. Brandner, and D. G. Braun.** 1984. Monoclonal antibodies against simian virus 40 nuclear large T tumour antigen: epitope mapping papova virus cross-reaction and cell surface staining. EMBO J. **3**:1485–1491.
3. **Birnboim, H. C.** 1983. A rapid alkaline extraction method for the isolation of plasmid DNA, p. 243–255. *In* R. Wu, L. Grossman, and K. Moldave (ed.), Methods in enzymology, vol. 100. Academic Press, Inc., New York.
4. **Blobel, G., and B. Dobberstein.** 1975. Transfer of proteins across membranes. II. Reconstitution of functional rough microsomes from heterologous components. J. Cell Biol. **67**:852–862.
5. **Bradley, M. K., J. Hudson, M. S. Villanueva, and D. M. Livingston.** 1984. Specific *in vitro* adenylation of the simian virus 40 large tumor antigen. Proc. Natl. Acad. Sci. USA **81**:6574–6578.
6. **Butel, J. S., and D. L. Jarvis.** 1986. The plasma-membrane-associated form of SV40 large tumor antigen: biochemical and biological properties. Biochim. Biophys. Acta **865**:171–195.
7. **Caliguiri, L. A., and I. Tamm.** 1970. The role of cytoplasmic membranes in poliovirus biosynthesis. Virology **42**:100–111.
8. **Chan, W.-K., M. E. Penaranda, S. E. Crawford, and M. K. Estes.** 1986. Two glycoproteins are produced from the rotavirus neutralization gene. Virology **151**:243–252.
9. **Chirgwin, J. M., A. E. Przybyla, R. J. MacDonald, and W. J. Rutter.** 1979. Isolation of biologically active ribonucleic acid from sources enriched in ribonuclease. Biochemistry **18**:5294–5299.
10. **Davis, L. I., and G. Blobel.** 1986. Identification and characterization of a nuclear pore complex protein. Cell **45**:699–709.
11. **Denhardt, D. T., and L. V. Crawford.** 1980. Simian virus 40 T-antigen: identification of tryptic peptides in the C-terminal region and definition of the reading frame. J. Virol. **34**:315–329.
12. **Deppert, W., and G. Walter.** 1982. Domains of simian virus 40 large T-antigen exposed on the cell surface. Virology **122**:56–70.
13. **Ericson, B. L., D. Y. Graham, B. B. Mason, and M. K. Estes.** 1982. Identification, synthesis, and modifications of simian rotavirus SA11 polypeptides in infected cells. J. Virol. **42**:825–839.
14. **Ericson, B. L., D. Y. Graham, B. B. Mason, H. H. Hanssen, and M. K. Estes.** 1983. Two types of glycoprotein precursors are produced by the simian rotavirus SA11. Virology **127**:320–332.
15. **Estes, M. K., and D. Y. Graham.** 1985. Rotavirus antigens, p. 201–214. *In* M. Z. Atassi and H. L. Bachrach (ed.), Advances in experimental medicine and biology, vol. 185. Immunobiology of proteins and peptides—III. Plenum Publishing Corp., New York.
16. **Estes, M. K., D. Y. Graham, R. F. Ramig, and B. L. Ericson.** 1982. Heterogeneity in the structural glycoprotein (VP7) of simian rotavirus SA11. Virology **122**:8–14.
17. **Estes, M. K., D. Y. Graham, E. M. Smith, and C. P. Gerba.** 1979. Rotavirus stability and inactivation. J. Gen. Virol. **43**:403–409.
18. **Gilmore, R., P. Walter, and G. Blobel.** 1982. Protein translocation across the endoplasmic reticulum. II. Isolation and characterization of the signal recognition particle receptor. J. Cell Biol. **95**:470–477.
19. **Gluzman, Y., and B. Ahrens.** 1982. SV40 early mutants that are defective for viral DNA synthesis but competent for transformation of cultured rat and simian cells. Virology **123**:78–92.
20. **Goldman, N., M. Brown, and G. Khoury.** 1981. Modification of SV40 T-antigen by poly-ADP-ribosylation. Cell **24**:567–572.
21. **Gooding, L. R., R. W. Gelb, K. A. O'Connell, and E. Harlow.** 1984. Antibody and cellular detection of SV40 T-antigen determinants on the surfaces of transformed cells, p. 263–269. *In* A. J. Levine, G. F. van de Woude, W. C. Topp, and J. D. Watson (ed.), Cancer cells, vol. 1. The transformed phenotype. Cold Spring Harbor Laboratory, Cold Spring Harbor, N.Y.
22. **Gooding, L. R., and K. A. O'Connell.** 1983. Recognition by cytotoxic T lymphocytes of cells expressing fragments of the SV40 tumor antigen. J. Immunol. **131**:2580–2586.
23. **Hanover, J. A., and W. J. Lennarz.** 1981. Transmembrane assembly of membrane and secretory glycoproteins. Arch. Biochem. Biophys. **211**:1–19.
24. **Holt, G. D., and G. W. Hart.** 1986. The subcellular distribution

of terminal N-acetylglucosamine moieties. Localization of a novel protein-saccharide linkage, O-linked GlcNAc. J. Biol. Chem. **261**:8049–8057.
25. **Holt, G. D., C. M. Snow, A. Senior, R. S. Haltiwar, L. Gerace, and G. W. Hart.** 1987. Nuclear pore complex glycoproteins contain cytoplasmically disposed O-linked N-acetylglucosamine. J. Cell Biol. **104**:1157–1164.
26. **Hunt, L. T., and M. O. Dayhoff.** 1970. The occurrence in proteins of the tripeptides Asn-X-Ser and Asn-X-Thr and of bound carbohydrate. Biochem. Biophys. Res. Commun. **39**: 757–765.
27. **Jarvis, D. L., and J. S. Butel.** 1985. Modification of simian virus 40 large tumor antigen by glycosylation. Virology **141**:173–189.
28. **Jarvis, D. L., C. N. Cole, and J. S. Butel.** 1986. Absence of a structural basis for intracellular recognition and differential localization of nuclear and plasma membrane-associated forms of simian virus 40 large tumor antigen. Mol. Cell. Biol. **6**:758–767.
29. **Jarvis, D. L., R. E. Lanford, and J. S. Butel.** 1984. Structural comparisons of wild-type and nuclear transport-defective simian virus 40 large tumor antigens. Virology **134**:168–176.
30. **Johnson, D. C., and M. J. Schlesinger.** 1980. Vesicular stomatitis virus and Sindbis virus glycoprotein transport to the cell surface is inhibited by ionophores. Virology **103**:407–424.
31. **Johnson, D. C., and P. G. Spear.** 1983. O-linked oligosaccharides are acquired by herpes simplex virus glycoproteins in the Golgi apparatus. Cell **32**:987–997.
32. **Kabcenell, A. K., and P. H. Atkinson.** 1985. Processing of the rough endoplasmic reticulum membrane glycoproteins of rotavirus SA11. J. Cell Biol. **101**:1270–1280.
33. **Kalderon, D., W. D. Richardson, A. F. Markham, and A. E. Smith.** 1984. Sequence requirements for nuclear localization of simian virus 40 large-T antigen. Nature (London) **311**:33–38.
34. **Kalderon, D., B. L. Roberts, W. D. Richardson, and A. E. Smith.** 1984. A short amino acid sequence able to specify nuclear location. Cell **39**:499–509.
35. **Karjalainen, H. E., M. J. Tevethia, and S. S. Tevethia.** 1985. Abrogation of simian virus 40 DNA-mediated transformation of primary C57BL/6 mouse embryo fibroblasts by exposure to a simian virus 40-specific cytotoxic T-lymphocyte clone. J. Virol. **56**:373–377.
36. **Kessler, S. W.** 1975. Rapid isolation of antigens from cells with a staphylococcal protein A-antibody adsorbent: parameters of the interaction of antibody-antigen complexes with protein A. J. Immunol. **115**:1617–1624.
37. **Klenk, H.-D., and R. Rott.** 1980. Cotranslational and posttranslational processing of viral glycoproteins. Curr. Top. Microbiol. Immunol. **90**:19–48.
38. **Klockmann, U., and W. Deppert.** 1983. Acylated simian virus 40 large T-antigen: a new subclass associated with a detergent-resistant lamina of the plasma membrane. EMBO J. **2**:1151–1157.
39. **Klockmann, U., and W. Deppert.** 1985. Evidence for transmembrane orientation of acylated simian virus 40 large T antigen. J. Virol. **56**:541–548.
40. **Kornfeld, R., and S. Kornfeld.** 1985. Assembly of asparagine-linked oligosaccharides. Annu. Rev. Biochem. **54**:631–664.
41. **Krieg, P. A., and D. A. Melton.** 1984. Functional messenger RNAs are produced by SP6 *in vitro* transcription of cloned cDNAs. Nucleic Acids Res. **12**:7057–7070.
42. **Lanford, R. E., and J. S. Butel.** 1979. Antigenic relationship of SV40 early proteins to purified large T polypeptide. Virology **97**:295–306.
43. **Lanford, R. E., and J. S. Butel.** 1982. Intracellular transport of SV40 large tumor antigen: a mutation which abolishes migration to the nucleus does not prevent association with the cell surface. Virology **119**:169–184.
44. **Lanford, R. E., and J. S. Butel.** 1984. Construction and characterization of an SV40 mutant defective in nuclear transport of T antigen. Cell **37**:801–813.
45. **Lanford, R. E., P. Kanda, and R. C. Kennedy.** 1986. Induction of nuclear transport with a synthetic peptide homologous to the SV40 T antigen transport signal. Cell **46**:575–582.
46. **Lanford, R. E., C. Wong, and J. S. Butel.** 1985. Differential ability of a T-antigen transport-defective mutant of simian virus 40 to transform primary and established rodent cells. Mol. Cell. Biol. **5**:1043–1050.
47. **Lange-Mutschler, J., and R. Henning.** 1984. Cell surface binding simian virus 40 large T antigen becomes anchored and stably linked to lipid of the target cells. Virology **136**:404–413.
48. **Mahin, D. T., and R. T. Lofberg.** 1966. A simplified method of sample preparation for determination of tritium, carbon-14, or sulfur-35 in blood or tissue by liquid scintillation counting. Anal. Biochem. **16**:500–509.
49. **Marchalonis, J. J., R. E. Cone, and V. Santer.** 1971. Enzymatic iodination: a probe for accessible surface proteins of normal and neoplastic lymphocytes. Biochem. J. **124**:921–927.
50. **Mason, B. B., D. Y. Graham, and M. K. Estes.** 1980. In vitro transcription and translation of simian rotavirus SA11 gene products. J. Virol. **33**:1111–1121.
51. **Mellor, A., and A. E. Smith.** 1978. Characterization of the amino-terminal tryptic peptide of simian virus 40 small-t and large-T antigens. J. Virol. **28**:992–996.
52. **Melton, D. A., P. A. Krieg, M. R. Rebagliati, T. Maniatis, K. Zinn, and M. R. Green.** 1984. Efficient *in vitro* synthesis of biologically active RNA and RNA hybridization probes from plasmids containing a bacteriophage SP6 promoter. Nucleic Acids Res. **12**:7035–7056.
53. **Morrison, T. G., and H. F. Lodish.** 1975. Site of synthesis of membrane and nonmembrane proteins of vesicular stomatitis virus. J. Biol. Chem. **250**:6955–6962.
54. **Noonan, C. A., J. S. Brugge, and J. S. Butel.** 1976. Characterization of simian cells transformed by temperature-sensitive mutants of simian virus 40. J. Virol. **18**:1106–1119.
55. **Noonan, C. A., and J. S. Butel.** 1978. Temperature-sensitive mutants of simian virus 40. I. Isolation and preliminary characterization of B/C gene mutants. Intervirology **10**:181–195.
56. **Olson, E. N., and G. Spizz.** 1986. Fatty acylation of cellular proteins. Temporal and subcellular differences between palmitate and myristate acylation. J. Biol. Chem. **261**:2458–2466.
57. **Oren, M., and A. J. Levine.** 1981. Immunoselection of simian virus 40 large T antigen messenger RNAs from transformed cells. Virology **113**:790–793.
58. **Paucha, E., R. Harvey, and A. E. Smith.** 1978. Cell-free synthesis of simian virus 40 T-antigens. J. Virol. **28**:154–170.
59. **Prives, C., E. Gilboa, M. Revel, and E. Winocour.** 1977. Cell-free translation of simian virus 40 early messenger RNA coding for viral T-antigen. Proc. Natl. Acad. Sci. USA **74**:457–461.
60. **Purchio, A. F., S. Jovanovich, and R. L. Erikson.** 1980. Sites of synthesis of viral proteins in avian sarcoma virus-infected chicken cells. J. Virol. **35**:629–636.
61. **Rigby, P. W. J., and D. P. Lane.** 1983. Structure and function of simian virus 40 large tumor antigen, p. 31–57. *In* G. Klein (ed.), Advances in viral oncology, vol. 3. Raven Press, New York.
62. **Robb, J. A., and K. Huebner.** 1973. Effect of cell chromosome number on simian virus 40 replication. Exp. Cell Res. **81**:120–126.
63. **Sabatini, D. D., G. Kreibich, T. Morimoto, and M. Adesnik.** 1982. Mechanisms for the incorporation of proteins in membranes and organelles. J. Cell Biol. **92**:1–22.
64. **Santos, M., and J. S. Butel.** 1984. Antigenic structure of simian virus 40 large tumor antigen and association with cellular protein p53 on the surfaces of simian virus 40-infected and -transformed cells. J. Virol. **51**:376–383.
65. **Santos, M., and J. S. Butel.** 1985. Surface T-antigen expression in simian virus 40-transformed mouse cells: correlation with cell growth rate. Mol. Cell. Biol. **5**:1051–1057.
66. **Scheidtmann, K.-H., B. Echle, and G. Walter.** 1982. Simian virus 40 large T antigen is phosphorylated at multiple sites clustered in two separate regions. J. Virol. **44**:116–133.
67. **Schickedanz, J., K.-H. Scheidtmann, and G. Walter.** 1986. Kinetics of nuclear transport and oligomerization of simian virus 40 large T antigen. Virology **148**:47–57.
68. **Schindler, M., M. Hogan, R. Miller, and D. DeGaetano.** 1987. A nuclear specific glycoprotein representative of a unique pattern of glycosylation. J. Biol. Chem. **262**:1254–1260.

69. **Schmidt, M. F. G.** 1983. Fatty acid binding: a new kind of posttranslational modification of membrane proteins. Curr. Top. Microbiol. Immunol. **102**:101–124.
70. **Schmidt-Ullrich, R., W. S. Thompson, S. J. Kahn, M. T. Monroe, and D. F. H. Wallach.** 1982. Simian virus 40 (SV40)-specific isoelectric point-4.7–94,000-Mr membrane glycoprotein: major peptide homology exhibited with the nuclear and membrane-associated 94,000-Mr SV40 T-antigen in hamsters. JNCI **69**:839–849.
71. **Schmieg, F. I., and D. T. Simmons.** 1984. Intracellular location and kinetics of complex formation between simian virus 40 T antigen and cellular protein p53. J. Virol. **52**:350–355.
72. **Schmitt, M. K., and K. Mann.** 1987. Glycosylation of simian virus 40 T antigen and localization of glycosylated T antigen in the nuclear matrix. Virology **156**:268–281.
73. **Sharma, S., L. Rodgers, J. Brandsma, M.-J. Gething, and J. Sambrook.** 1985. SV40 T antigen and the exocytic pathway. EMBO J. **4**:1479–1489.
74. **Shields, D., and G. Blobel.** 1978. Efficient cleavage and segregation of nascent presecretory proteins in a reticulocyte lysate supplemented with microsomal membranes. J. Biol. Chem. **253**:3753–3756.
75. **Soule, H. R., and J. S. Butel.** 1979. Subcellular localization of simian virus 40 large tumor antigen. J. Virol. **30**:523–532.
76. **Soule, H. R., R. E. Lanford, and J. S. Butel.** 1982. Detection of simian virus 40 surface-associated large tumor antigen by enzyme-catalyzed radioiodination. Int. J. Cancer **29**:337–344.
77. **Stinebaugh, S., and J. L. Melnick.** 1962. Plaque formation by vacuolating virus, SV40. Virology **16**:348–349.
78. **Tartakoff, A. M.** 1983. Perturbation of vesicular traffic with the carboxylic ionophore monensin. Cell **32**:1026–1028.
79. **Tegtmeyer, P., K. Rundell, and J. K. Collins.** 1977. Modification of simian virus 40 protein A. J. Virol. **21**:647–657.
80. **Tooze, J. (ed.).** 1981. Molecular biology of tumor viruses, 2nd ed., part 2. DNA tumor viruses, p. 61–338. Cold Spring Harbor Laboratory, Cold Spring Harbor, N.Y.
81. **Torres, C.-R., and G. W. Hart.** 1984. Topography and polypeptide distribution of terminal N-acetylglucosamine residues on the surfaces of intact lymphocytes. Evidence for O-linked GlcNAc. J. Biol. Chem. **259**:3308–3317.
82. **Van Roy, F., L. Fransen, and W. Fiers.** 1983. Improved localization of phosphorylation sites in simian virus 40 large T antigen. J. Virol. **45**:315–331.
83. **Walter, P., and G. Blobel.** 1980. Purification of a membrane-associated protein complex required for protein translocation across the endoplasmic reticulum. Proc. Natl. Acad. Sci. USA **77**:7112–7116.
84. **Walter, P., R. Gilmore, and G. Blobel.** 1984. Protein translocation across the endoplasmic reticulum. Cell **38**:5–8.
85. **Whittaker, L., A. Fuks, and R. Hand.** 1985. Plasma membrane orientation of simian virus 40 T antigen in three transformed cell lines mapped with monoclonal antibodies. J. Virol. **53**:366–373.
86. **Wickner, W. T., and H. F. Lodish.** 1985. Multiple mechanisms of protein insertion into and across membranes. Science **230**:400–407.
87. **Zilberstein, A., M. D. Snider, M. Porter, and H. F. Lodish.** 1980. Mutants of vesicular stomatitis virus blocked at different stages in maturation of the viral glycoprotcin. Cell **21**:417–427.